J. Serb. Chem. Soc. 91 (0) 1–16 (2026)
JSCS–13681

Original scientific paper
Published 00 MM, 2026

Impact of silica gel G on mechanical and microstructural properties of magnesium oxychloride

NISHA YADAV[1], BHUPENDRA PAL[2] and MEENAKSHI[1]*

[1]*Department of Chemistry, University of Rajasthan, Jaipur, Rajasthan,302004, India and* [2]*Government Polytechnic College, Karauli, Rajasthan, 322241, India*

(Received 17 December 2025, revised 19 January, accepted 21 April 2026)

Abstract: Magnesium oxychloride cement (MOC), a type of Sorel's cement, has gained renewed attention as a sustainable building material due to its low carbon footprint and energy consumption. However, its application in construction remains limited, primarily due to its inadequate moisture resistance and reduced early-age strength under elevated temperature conditions. This research investigates the impact of silica gel G (SG) on the properties of MOC. SG was incorporated into MOC at varying proportions (0–20 wt. % MgO) to form MOC–SG composites. The study evaluated the physical and mechanical properties of these composites, including setting time, moisture ingress resistance and compressive strength. Additionally, FTIR, PXRD, SEM-EDX and TGA analyses were conducted to examine the crystalline phases of the composites. SG acts as a binding agent, enhancing the strength and durability of the composite. This research demonstrates the potential of MOC–SG composites as promising sustainable building material. Results indicate that the addition of 5 % SG significantly improves the properties of MOC.

Keywords: cement; silica gel G; setting time; water resistance; compressive strength.

INTRODUCTION

Cement, a foundational material in human civilization and infrastructure development, has been utilized for centuries.[1] In recent years, there has been a growing interest in low-carbon cement alternatives, such as magnesium oxide-based cement. Magnesium oxychloride cement (MOC) was first developed in 1867 by Sorel.[2] In recent years, MOC is gaining attention due to its low energy consumption and reduced CO_2 emissions.[3–7]

In comparison with ordinary Portland cement (OPC), MOC exhibits several noteworthy performance advantages, including high early and ultimate strength,

* Corresponding author. E-mail: meenakshialwaraj@gmail.com
https://doi.org/10.2298/JSC251217021Y

strong interfacial bonding, rapid setting, low thermal conductivity, enhanced wear resistance, favorable mechanical properties, dimensional stability and excellent cohesiveness in lightweight composite panels.[8,9] Additionally, its inherent fire resistance and the absence of the requirement for humid curing further contribute to its applicability across diverse construction contexts.[10]

MOC is frequently referred to as a green or eco-friendly cement due to its lower energy demand during synthesis, requiring neither high-temperature processing nor external heat or light. The CO_2 emissions associated with MOC production are typically 40–50 % lower than those associated with OPC. Moreover, MOC continues to sequester CO_2 from the atmosphere after curing and does not release heat during curing, making it a viable and cost-effective substitute for energy-intensive OPC.

MOC is produced through the direct reaction between lightly calcined MgO and a concentrated $MgCl_2$ solution. This reaction is exothermic and the heat generated can induce microcracking during the setting and curing stages. Such thermal microcracks facilitate water ingress, ultimately compromising the compressive strength and durability of the cement. To mitigate this issue, an inert filler is incorporated into the MOC matrix. Acting through a collision-based heat absorption mechanism, this filler dissipates thermal energy without participating in the primary cementation reactions.[11] In the present study, dolomite powder was used as an inert filler to decrease thermal shock and minimize crack development in MOC:

$$\mathrm{MgO(s)} + \mathrm{MgCl_2 \cdot 6H_2O(liq.)} \rightarrow \mathrm{MOC} + \mathrm{Heat} \rightarrow \mathrm{Cracking} \quad (1)$$

$$\mathrm{MgO(s)} + \mathrm{MgCl_2 \cdot 6H_2O(liq.)} + \mathrm{Inert\ filler} \rightarrow \mathrm{(No\ cracking)} \rightarrow \mathrm{MOC} + \mathrm{Inert\ filler^*} \quad (2)$$

Temperature, along with the mole ratios and relative concentrations of MgO, $MgCl_2$ and H_2O, plays a critical role in governing the hydration and mineral composition of MOC. These parameters strongly influence the formation, stability and proportion of hydration products, typically represented as $x\mathrm{Mg(OH)_2} \cdot y\mathrm{MgCl_2} \cdot z\mathrm{H_2O}$, which in turn exert a direct effect on the resulting compressive strength of the material.[12,13]

Several distinct phase assemblages are known to form within the MgO––$MgCl_2$–H_2O system, including phase-3 ($3\mathrm{Mg(OH)_2} \cdot \mathrm{MgCl_2} \cdot 8\mathrm{H_2O}$), phase-5 ($5\mathrm{Mg(OH)_2} \cdot \mathrm{MgCl_2} \cdot 8\mathrm{H_2O}$), phase-9 ($9\mathrm{Mg(OH)_2} \cdot \mathrm{MgCl_2} \cdot 8\mathrm{H_2O}$) and phase-2 ($2\mathrm{Mg(OH)_2} \cdot \mathrm{MgCl_2} \cdot 8\mathrm{H_2O}$), which are typically stable over temperatures ranging from approximately 30 to 120 °C. The specific hydrate phases present in the hardened matrix are largely determined by the $MgO/MgCl_2$ mole ratio, which controls the reaction pathways and ultimate phase composition.

Under ambient conditions, phase-5 and phase-3 are the predominant and most thermodynamically stable hydration products in MOC systems, as represented in reactions (3) and (4):

$$5MgO + MgCl_2 + 13H_2O \rightarrow 5Mg(OH)_2 \cdot MgCl_2 \cdot 8H_2O \text{ (Phase-5)} \quad (3)$$

$$3MgO + MgCl_2 + 11H_2O \rightarrow 3Mg(OH)_2 \cdot MgCl_2 \cdot 8H_2O \text{ (Phase-3)} \quad (4)$$

These phases contribute significantly to strength development, durability and overall performance of MOC.

Although MOC exhibits a wide range of favorable mechanical and engineering properties, its large-scale industrial application remains significantly constrained. The primary limitations arise from its poor resistance to moisture and its susceptibility to reduced early-age strength when exposed to elevated temperatures. These drawbacks lead to excessive moisture uptake, dimensional instability and structural deformability under humid or high-temperature conditions. Consequently, despite its promising performance attributes, the broader commercial adoption of MOC has been limited. Owing to its many advantageous characteristics, extensive research has been devoted to magnesium oxychloride cement, with numerous studies aiming to further enhance its performance and broaden its applicability. A wide range of inorganic, organic, and hybrid additives have been incorporated into MOC systems with the aim of enhancing properties such as moisture resistance, mechanical strength, dimensional stability and overall durability.[14–25]

Numerous studies have demonstrated that incorporating silica-based materials such as silica fume, nano-silica and others, either individually or in combination with supplementary additives like fly ash and phosphoric acid, significantly enhances the water resistance and overall performance of MOC. Silica fume, owing to its ultrafine particle size and high amorphous SiO_2 content, improves MOC mainly by filling micropores, microstructure densification and promoting the formation of magnesium–silicate–hydrate or Mg–Cl–Si–H type gels, which have superior stability in moist environments compared with conventional MOC hydration phases.[26] Hybrid systems incorporating silica fume and fly ash often demonstrate synergistic effects, with improved long-term retention of strength after water immersion while maintaining adequate mechanical properties.[27,28] Nano-silica, owing to its high reactivity and surface area, further accelerates hydration, promotes secondary reactions of unreacted MgO, refines the pore structure and markedly reduces permeability. These effects translate into notable improvements in compressive strength and durability under wet conditions.[29] When nano-silica is combined with fly ash or phosphate-based modifiers, additional improvements arise owing to the formation and stabilization of water-resistant binding gels.[30] Collectively, the literature indicates that silica-based additives play a crucial role in mitigating the inherent water sensitivity of MOC by altering its hydration chemistry and microstructure.

Silica gel G (SG) is an amorphous form of SiO_2 containing approximately 13 % gypsum, which contributes to its binding capability. This research study aims to introduce SG as a novel additive for MOC and evaluate its effect on the material's

physicochemical and mechanical properties. The investigation also examines dolomite as an inert filler alongside SG, considering its role in improving particle packing, dimensional stability and resistance to shrinking-induced microcracking. The key objective is to determine whether the combined use of SG and dolomite can refine the MOC microstructure, lower capillary porosity, stabilize hydration products, and promote water-resistant binding phases, thereby improving durability and reducing the well-known susceptibility of MOC to strength loss under water exposure.

EXPERIMENTAL

Materials

In this study, magnesium oxide (MgO), magnesium chloride ($MgCl_2 \cdot 6H_2O$), dolomite and silica gel G (SG) were used as the raw materials.

*Magnesium ox*ide. Lightly calcined commercial grade MgO was procured from Suksha Exports, Jaipur, Rajasthan, India. The chemical composition of MgO was: MgO = 89.90 %, SiO_2 = 4.19 %, CaO = 1.40 %, Fe_2O_3 = 0.12 % and Al_2O_3 = 0.88 %. The loss of ignition, brightness and whiteness of MgO were 3.08, 88.20 and 91.60 %, respectively.[31]

Magnesium chloride (as $MgCl_2.6H_2O$). Technical grade magnesium chloride was procured from Alum Scientific Suppliers, Jaipur, Rajasthan, India. It is a colorless crystalline and hygroscopic compound, which has a purity of 96.60 %.[32]

Dolomite. In this study, commercial grade dolomite was used as an inert filler and procured from Ases Chemical Works, Jodhpur, Rajasthan, India. The chemical composition of dolomite was: CaO = 28.00 %, MgO = 18.00 %, SiO_2 = 10.98 %, Fe_2O_3 = 0.71 % and Al_2O_3 = 0.10 %. The *LOI*, brightness and whiteness of dolomite were 41.80, 89.40 and 92.70 %, respectively.[33]

Silica Gel G. In this study, SG was employed as a chemical admixture and procured from CDH Fine Chemicals, New Delhi, India.

Methods

The methods for the preparation of the dry-mix composition, the gauging solution and the wet-mix composition with the incorporation of SG are as fllows.

Preparation of dry-mix composition and incorporation of silica gel G. To prepare the dry--mix, MgO and dolomite were gently mixed together in an equal weight ratio. Powdered SG was also mixed into this dry-mix composition in varying weight proportions of 5, 10, 15 and 20 % with respect to MgO. A control dry-mix was also prepared with no addition of SG.

Preparation of gauging solution. To prepare the gauging solution, a sufficient amount of $MgCl_2 \cdot 6H_2O$ powder was added to lukewarm water (37 °C) with continuous agitation until saturation point was reached. This saturated solution of $MgCl_2$ is referred to as the gauging solution for MOC. The concentration of saturated gauging solution was obtained approx. 31 °Be on Baume Scale. A solution of $MgCl_2 \cdot 6H_2O$ of 25 °Be concentration was used as the gauging solution in the present research work.

Preparation of wet-mix. To form the wet-mix, the gauging solution was blended into the dry-mix to get a workable wet-mix consistency. The incorporation of SG into the optimal cementing composition of MOC was investigated with this wet-mix composition. To obtain a uniform and workable paste, the solid-to-solution ratio was optimized experimentally for each mix. For the compressive-strength specimens, the total solid mass (MgO + dolomite) was fixed at 540 g (MgO:Dolomite = 1:1) for compressive strength analysis (Table S-1 of the Supplementary

material to this paper) and at 200 g (MgO:dolomite = 1:1) for setting time analysis, and the volume of $MgCl_2$ solution required for workable consistency varied with the SG content (Table S-II of the Supplementary material).

In this study, each experimental procedure was repeated five times and the average value was taken into account to get accurate readings. All experiments were performed under controlled environmental conditions, maintaining a constant temperature of 30 °C and a relative humidity of approximately 90 % throughout the testing period.

Following procedures were conducted to investigate the effect of SG in MOC.

Setting time investigation

To evaluate the effect of SG on setting characteristics of MOC, different percentages (5, 10, 15 and 20 %) of SG were mixed with dry-mix composition (MgO:dolomite = 1:1) in varying proportions. This mixture was then gauged with gauging solution to form a workable wet-mix. A standard procedure was adopted according to the Indian Standard (IS 10132-1982) specification to determine standard consistency. A Vicat needle apparatus was used to determine the initial and final setting times.[33] Setting time blocks of simple MOC (M0, only MgO and gauging solution) and control MOC (M1, MgO:dolomite = 1:1 with gauging solution) were also prepared for comparative analysis. Results are reported in Fig. 1.

Water ingress investigation

Moisture ingress tests were conducted on all previously prepared setting-time specimens to assess the effect of SG on the soundness of MOC. After a curing period of 60 days, the specimens (M0, M1 and various MOC–SG formulations) were subjected to boiling-water exposure, a procedure essential for evaluating their comparative moisture-sealing performance. A time-dependent assessment was then performed to determine the relative moisture resistance of each composition at successive intervals across a total duration of 30 h. The measurements were recorded at the time intervals of 0–5, 5–10, 10–15, 15–20, 20–25 and 25–30 h, to systematically monitor the progressive changes in the system. The comparative results of moisture-resistance performance for all specimens are summarized in Table S-III of the Supplementary material.

Compressive strength

To evaluate the influence of SG on the compressive strength of MOC, standard cube specimens of dimensions of 70.6 mm×70.6 mm×70.6 mm with a surface area of 50 cm^2 were fabricated using various compositions (M0, M1 and MOC–SG formulations containing 5, 10, 15 and 20 % of SG).[33] The dry mixtures were homogenized and subsequently gauged with the prepared gauging solution before being cast into molds. After remaining in the molds for 24 h, the specimens were demolded and subjected to a 28-day curing period under controlled environmental conditions (temperature around 30 °C, and relative humidity above 90 %). Compressive strength testing was performed using a universal testing machine in accordance with standard procedures (Fig. S-3 of the Supplementary material). The results of the compressive strength measurements are presented in Fig. 2.

Spectroscopic analysis

The effect of SG on the MOC block was also investigated through the following spectroscopic techniques using the best modified MOC–SG composite.

Fourier transform-infrared spectroscopy (FT-IR). FT-IR spectra of MOC and SG-incorporated MOC–SG composite cement were recorded using an MRC-28 FT-IR analyzer in the range from 400 to 4000 cm^{-1}. For FT-IR analysis, the MOC cement samples were prepared in dehydrated potassium bromide.

Powder X-ray diffraction (PXRD). PXRD diffraction patterns of MOC and SG-incorporated MOC–SG composite cement were recorded using a Panalytical X Pert Pro Diffractometer (conditions for diffraction pattern: 2θ 5–70°, CuKα radiation, λ = 0.15406 Å).

Microscopic analysis

Field emission-scanning electron microscopy (FE-SEM) images of MOC and SG-incorporated MOC–SG composite were recorded using a Jeol JSM- 7610F Plus FE-SEM Instrument. An EDS was also performed for elemental analysis of MOC and MOC––SG composite samples.

Thermogravimetric analysis

Thermogravimetric analysis (TGA) of MOC and SG-incorporated MOC–SG composite cement was performed using a Perkin Elmer STA 6000 to evaluate the thermal stability. MOC and MOC–SG composite samples were heated under a nitrogen environment from room temperature to 800 °C at a rate of 10 °C per min to obtain the results.

RESULTS AND DISCUSSION

Setting time analysis

Fig. 1 illustrates the influence of varying SG concentrations (0–20 %) on the initial and final setting times of the resulting composites. The exothermic reaction between MgO and the $MgCl_2$ solution is responsible for the rapid setting of MOC. Hence the shortest initial and final setting times were observed for M0 without dolomite and additive.

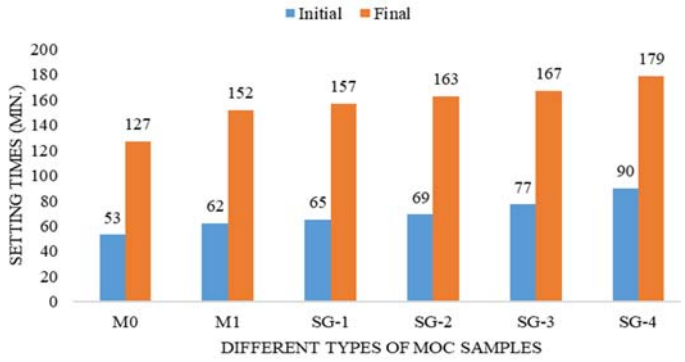

Fig. 1. Setting times of M0, M1, and different types of MOC-SG samples; M0 = MgO + gauging solution; M1 = (MgO:dolomite = 1:1) + gauging solution; SG-1 = (MgO:dolomite = 1:1) + 5% SG + gauging solution; SG-2 = (MgO:dolomite = 1:1) + 10 % SG + gauging solution; SG-3= (MgO:dolomite = 1:1) + 15% SG + gauging solution; SG-4 = (MgO:dolomite = 1:1) + 20 % SG + gauging solution.

In contrast, the control sample (M1) with 50 % dolomite replacement exhibited relatively longer setting time than M0 due to the reduced exothermic reaction. Dolomite works as an inert filler, being responsible for absorption of thermal

shocks *in situ* in MOC by the three-body collision mechanism, as represented in reactions (1) and (2).

However, the addition of SG, a hydrophilic material, delays the setting process. SG's strong hydrogen bonding capacity leads to increased water retention, hindering the hydration reaction and extending both the initial and final setting times. As the SG concentration rises, the water retention capacity increases, further delaying the setting process and leading to a more controlled setting profile.

Analysis of water resistance

The water resistance characteristics of the MOC specimens are presented in Table S-III. Owing to the highly exothermic reaction between magnesium oxide and the magnesium chloride solution, visible cracks developed in the M0 sample during the curing stage (Fig. S-1). During the subsequent water-resistance test, these cracks facilitated rapid water penetration, leading to their further widening and propagation. The increased permeability significantly accelerated water absorption and consequently diminished the overall water resistance of the M0 composition, rendering it unsuitable for structural applications.

In contrast, neither the M1 sample nor the SG-modified MOC specimens exhibited cracking during curing (Fig. S-2). The improved resistance to crack formation and water absorption can be attributed to the presence of dolomite, which effectively absorbs a portion of the heat generated during the exothermic reaction of the reactive components. By moderating the temperature rise, dolomite limits internal stress development and prevents crack initiation. The absence of cracks significantly restricts water ingress, thereby enhancing the overall durability of the cement matrix. Furthermore, dolomite contributes to improved water resistance by occupying internal voids and micropores within the hardened matrix. This pore-filling effect reduces the permeability of the cement, impeding water migration through the material and promoting the formation of a denser and more structurally sound matrix.

Compressive strength analysis. Fig. 2 illustrates the compressive strength of MOC–SG composite blocks after a 28-day air curing period. The M0 sample, exhibited significant cracking during curing due to the exothermic reaction between MgO and $MgCl_2$, rendering it unsuitable for construction applications (Fig. S-1). The M1 sample and different types of SG samples were free from cracks due to the presence of dolomite (Fig. S-2). The addition of SG resulted in a notable enhancement in the compressive strength of the composite blocks. Specifically, the SG-1 sample demonstrated the highest compressive strength, surpassing both the control sample (M1) and samples with higher SG concentrations. The strong hydrogen bonding between the hydroxyl groups of SG and the MOC matrix likely contributed to the formation of interlocking crystals, leading to improved mechanical properties. However, excessive SG incorporation was found to be detrimental

to the compressive strength. Therefore, the optimal SG concentration for enhancing the mechanical properties of MOC–SG composites was determined to be 5 % by weight of MgO. Building upon the physical analysis results, M1 and SG-1 composite blocks were subjected to in-depth characterization using FT-IR and PXRD spectroscopic analyses.

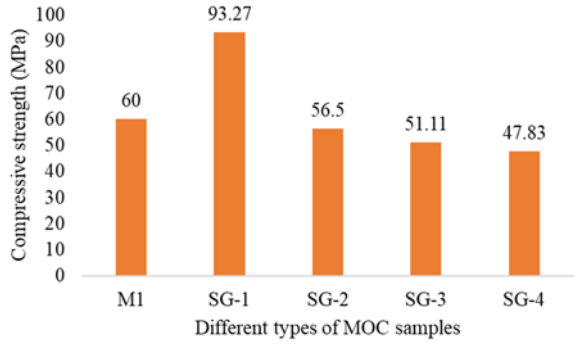

Fig. 2. Effect of silica gel G on compressive strength characteristics of MOC–SG composite blocks.

FT-IR analysis. FT-IR spectra of both M1 and SG-1 composite samples were recorded using KBr pellets in the range of 400–4000 cm^{-1} at ambient conditions. Fig. 3 illustrates the FT-IR spectra of M1 and SG-1. Both M1 and SG-1 exhibited sharp, intense peaks in the 3600–3800 cm^{-1} region, characteristic of the stretching vibrations of water molecules.[34,35] However, the incorporation of SG resulted in broader, less intense peaks in this range, indicating a decrease in water content. This suggests that SG enhances the water resistance of the MO–SG composite. The stretching vibrations of crystalline hydroxyl groups were observed at 3695 (M1) and 3698 cm^{-1} (SG-1), which are attributed to the stretching vibrations of the –OH group in brucite ($Mg(OH)_2$) and suggest a low presence of $Mg(OH)_2$ in both samples. This is beneficial for the mechanical strength and moisture resistance of the SG-1 composite sample.

The peaks at 1622 (M1), 1611 (SG-1), 3435 (M1) and 3428 cm^{-1} (SG-1) originate from the crystalline phases, specifically phase-5 ($5Mg(OH)_2{\cdot}MgCl_2{\cdot}8H_2O$) and phase-3 ($3Mg(OH)_2{\cdot}MgCl_2{\cdot}8H_2O$), of the MOC matrix. The peak at 1385 cm^{-1} corresponds to the linear C–O bond vibration in carbonates. The peak at 1445 (M1) and 1439cm^{-1} (SG-1) associated with asymmetric C=O stretching, becomes broader and more intense in SG-1, indicating an interaction between the polar C=O group and the functional groups of SG. The out-of-plane bending of CO_3^{2-} is represented by peaks at 881 (SG-1) and 880 cm^{-1} (M1).[3] The absorption bands at 726 and 730 cm^{-1} (M1 and SG-1), 530 (SG-1) and 542 cm^{-1} (M1), are attributed to the stretching and bending vibrations of Si–O, Mg–O and Mg–Cl, respectively.

Peaks at 1611 (SG-1) and 1622 cm^{-1} (M1) can be attributed to O–H bending vibrations. The presence of dolomite is also shown by the carbonate absorption peak at 2530 (SG-1) and 2527 cm^{-1} (M1). The reduction in O–H peak intensity suggests the formation of hydrogen bonds between the hydroxyl groups of MOC phases and silica gel G. This hydrogen bonding, facilitated by SG, creates a protective coating that enhances the bonding strength of the MOC.

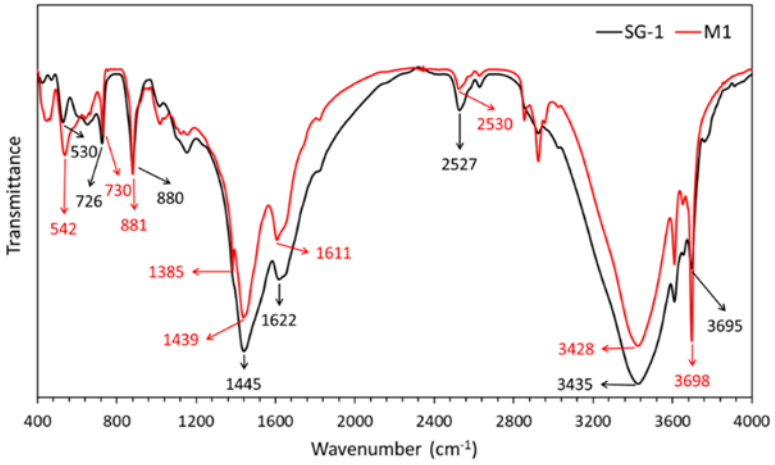

Fig. 3. FT-IR spectra of M1 and silica gel G (SG) incorporated SG-1 composite samples.

Powdered XRD analysis. PXRD spectra of M1 and SG-1 composite samples were recorded at ambient conditions and are presented in Fig. 4. As evidenced by the diffraction patterns, the primary components of the MOC cement are phase-5 ($5Mg(OH)_2 \cdot MgCl_2 \cdot 8H_2O$), unreacted MgO, brucite and minor carbonated MgO. The characteristic reflections of MgO are indicated by peaks at 2θ 43 and 62.5°, indicating incomplete MgO hydration in both systems. The incorporation of 5 % SG does not significantly introduce any new crystalline phases into the MOC composite matrix. The overall phase assemblage of SG-1 remains similar to that of M1, indicating that SG does not participate in crystallization as a distinct crystalline phase. However, a noticeable change in peak characteristics is observed. Compared to M1, SG 1 pattern exhibits slightly reduced peak intensities accompanied by moderate peak broadening, which suggests refinement of the crystalline size and/or an increase in structural disorder. These changes are consistent with a modification of the hydration and crystallization process rather than a change in phase composition.

A particularly prominent peak at 2θ 31°, associated with the inert filler dolomite, is present in both samples with comparable intensity. This suggests that dolomite remains unreactive during hydration and functions as a heat-absorbing filler, without participating in the formation of hydration products. No distinct dif-

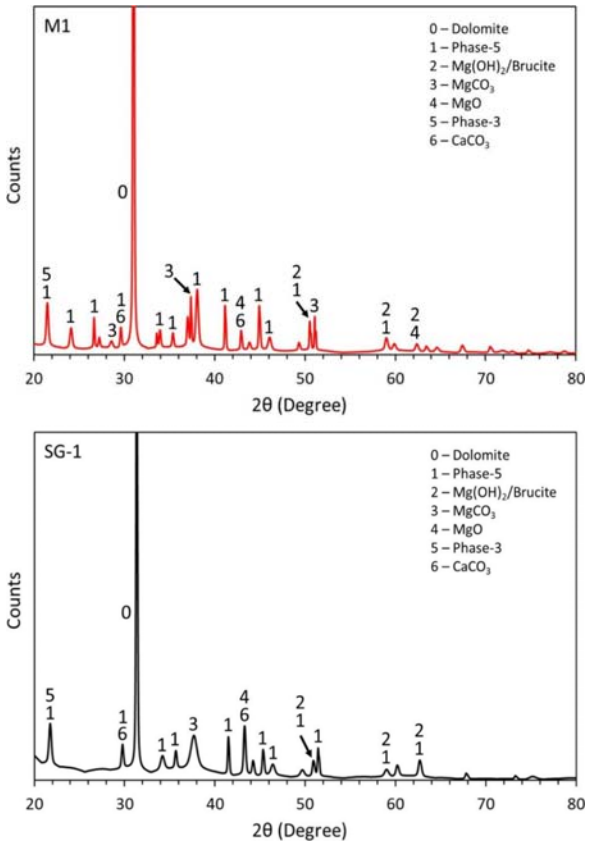

Fig. 4. PXRD spectra of M1 and SG-1 samples.

fraction peaks attributable to SG are detected in SG-1. This observation is expected, as SG is predominantly amorphous in nature and therefore does not contribute sharp crystalline reflections in PXRD. The absence of additional peaks also confirms that SG does not form new crystalline reaction products with the MOC phases within the detection limits of PXRD. Instead, its presence is suggested to influence the nucleation and growth kinetics of phase-5, which is also supported by the observed extension in setting time. The qualitative comparison of peak positions and relative intensities suggests that the incorporation of SG modifies the microstructural packing and crystallization behavior of the MOC matrix. This microstructural refinement is consistent with the experimentally observed improvements in water resistance and thermal stability of SG-1. The mechanical enhancement observed for SG-1 is therefore attributed to microstructural densification and improved phase interlocking, rather than an increase in the absolute amount of phase-5.

343 *SEM-EDX analysis*. SEM-EDX analyses of both M1 and SG-1 were recorded
344 and are shown in Figs. 5 and 6. The incorporation of silica gel G helped the rod-
345 -like phase-5 crystals (M1) convert into a gel-like amorphous phase-5 structure
346 (SG-1), which could notably reinforce the mechanical properties. It is also clear
347 that the needle-like shape of the crystals was clearer in the SG-1 composite mat-
348 erial than in M1. Due to the needle-like crystals, SG-1 exhibited more interlocking

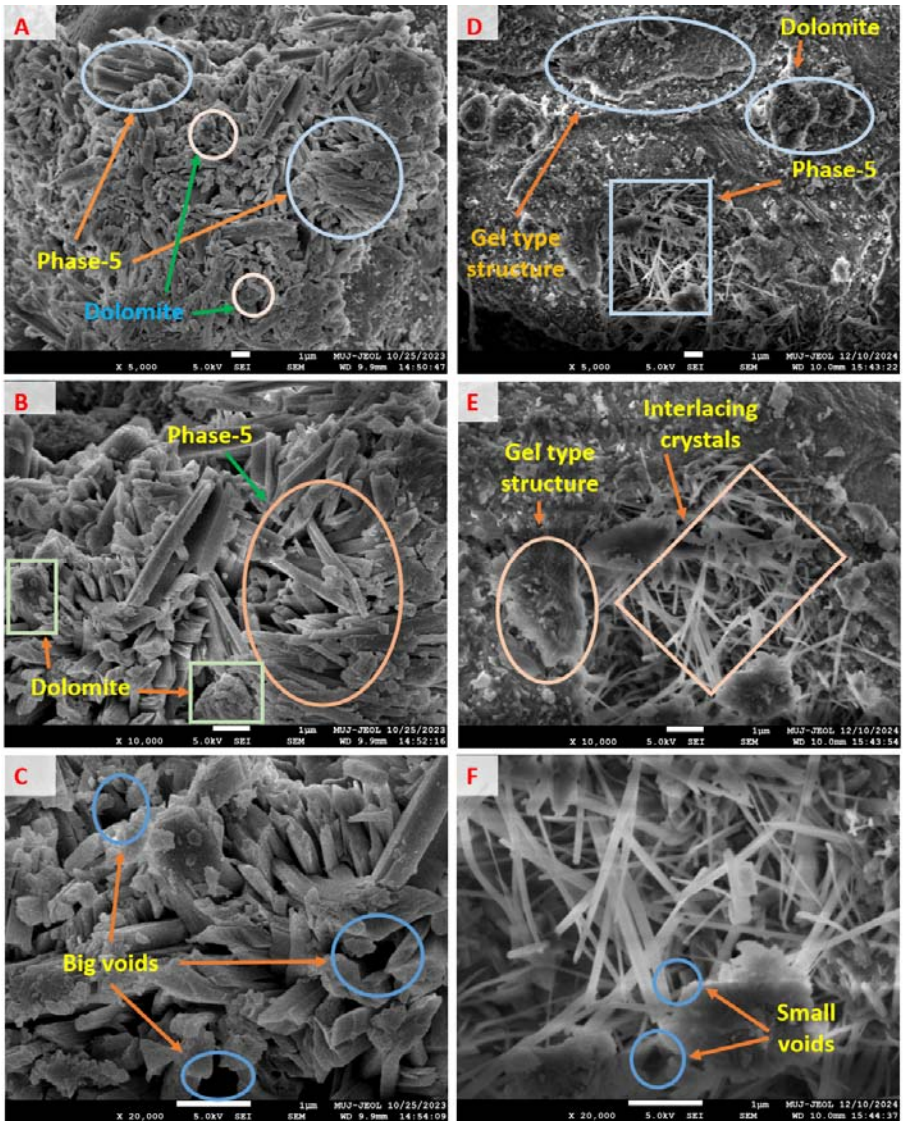

Fig. 5. SEM images of M1 (A–C) and SG-1 (D–F) MOC-SG composite samples at different magnifications.

phase-5, which can be explained by the smaller void gaps in SG-1 composite (Fig. 5F) as compared to the larger void gaps in M1 (Fig. 5C). Therefore, SG-1 showed more interlocking phase-5 than M1, supporting enhanced strength and durability. In addition, the transformation of phase-5 resulted in smaller voids in SG-1, thereby increasing the water-resistance of MOC.

The SEM–EDX analysis (Fig. 6) shows distinct differences in the elemental ratios of Mg, Cl and O between M1 and SG-1. The mole ratio in M1 is 10.45:1.00:28.59, whereas SG-1 exhibits a ratio of 1.13:1.00:2.41. Rather than indicating the presence of amorphous phases, these differences reflect the relative proportions of magnesium-chloride-based hydration products formed in each mix. The higher Mg and Cl content in SG-1 suggests a greater formation of phase-5-type MOC hydration products, consistent with the known role of silica additives in promoting phase-5 development. This interpretation is in agreement with literature reports, which demonstrate that silica gel enhances both the quantity and crystallite size of phase-5.[35] In contrast, the higher oxygen proportion in M1 is attributed to the larger amount of carbonate minerals present in the mix, rather than to any amorphous hydration product.

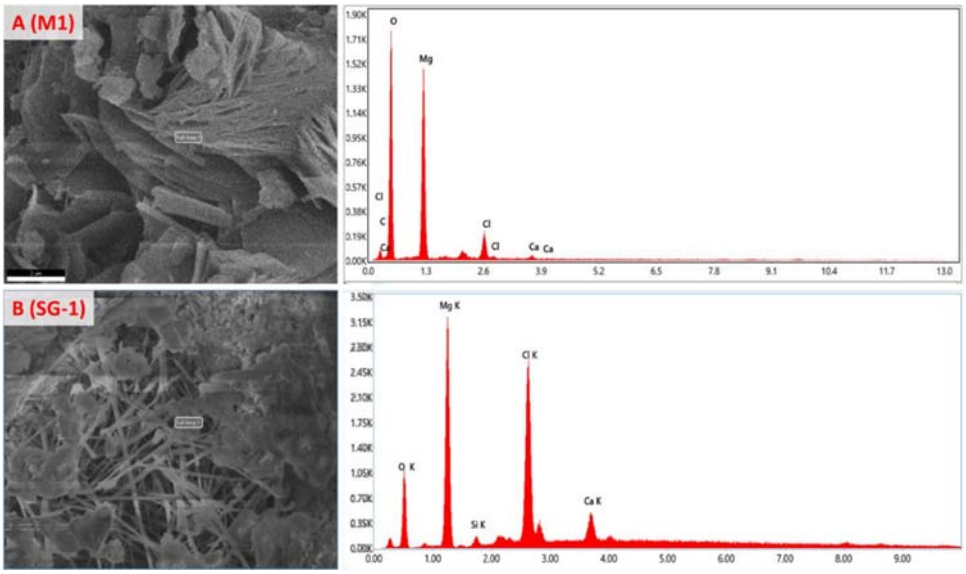

Fig. 6. SEM-EDX of M1 (A) and SG-1 (B) MOC–SG composite samples.

Thermogravimetric analysis. The thermal decomposition of M1 and SG-1 can be seen from the TGA curves in Fig. 7. The decomposition takes place in three stages (Eqs. (5)–(7)). Both M1 and SG-1 samples exhibit mass loss as a result of the slow evaporation of moisture (free water molecules), crystalline water, structural water and hydrochloric acid content throughout the heating process.[36,37]

The weight loss in the first stage is nearly the same in both M1 and SG-1 samples, but slightly less weight loss was observed in SG-1. In the second stage, the weight loss increases in both M1 and SG-1 compared to the first stage weight loss and M1 exhibits greater weight loss compared to SG-1. In the third stage, the weight loss decreases as compared to both the first and second stages in M1. SG-1 has comparatively more weight loss in third stage as compared to M1. It was indicated that SG-1 is more thermally stable in the lower temperature range (30 to 430 °C), but undergoes rapid decomposition in the temperature range of 430–730 °C and becomes constant after 730 °C. The overall weight loss in M1 and SG-1 is 44.80 and 38.04 %, respectively, and therefore, SG-1 sample is thermally more stable than M1:

$$5MgO(OH)_2 \cdot MgCl_2 \cdot 8H_2O \rightarrow 5Mg(OH)_2 \cdot MgCl_2 \cdot 8H_2O \quad (5)$$

$$5Mg(OH)_2 \cdot MgCl_2 \rightarrow MgCl_2 \cdot H_2O + 5MgO \quad (6)$$

$$MgCl_2 \cdot H_2O \rightarrow MgO + 2HCl \quad (7)$$

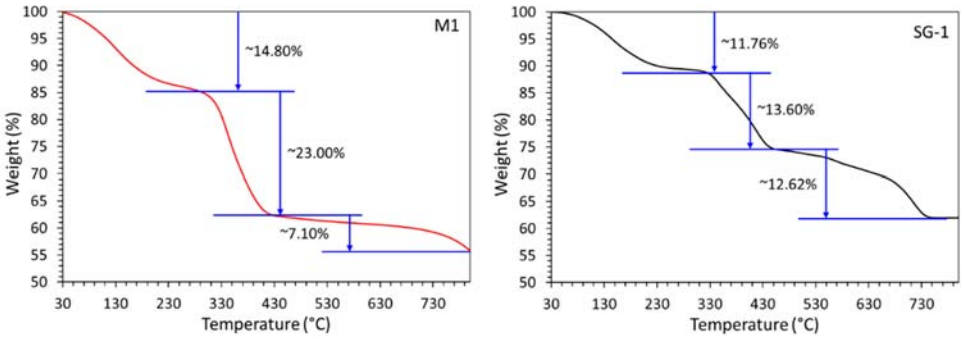

Fig. 7. TGA of M1 and SG-1 sample.

CONCLUSION

This research investigated the potential of silica gel G as an additive in magnesium oxychloride cement to enhance its properties and sustainability. The incorporation of SG in varying proportions (0–20 % by weight of MgO) led to notable improvements in the physical and mechanical properties of the resulting MOC––SG composites. The mixing of SG into MOC significantly enhanced its physical and mechanical properties.

The key findings include:

Accelerated setting time; the addition of SG reduced the initial and final setting time of MOC, likely due to the decreased availability of MgO for the hydration reaction.

Enhanced mechanical strength; SG contributed to an increase in the compressive strength of MOC–SG composites, reaching an optimum value at around 5 % SG content. This improvement is attributed to the formation of additional hydration products and the filling of pores by SG particles.

Improved thermal stability; the incorporation of SG enhanced the thermal stability of MOC–SG composites. This is likely due to the formation of a more stable crystalline structure and the reduced porosity of the composite.

Overall, the results of this study demonstrate the potential of silica gel G as a valuable additive for improving the performance of magnesium oxychloride cement. Further research is recommended to optimize the dosage of silica gel G and explore its impact on other properties, such as durability and fire resistance.

SUPPLEMENTARY MATERIAL

Additional data and information are available electronically at the pages of journal website: https://www.shd-pub.org.rs/index.php/JSCS/article/view/13681, or from the corresponding author on request.

Acknowledgements. The authors are thankful to Department of Chemistry, University of Rajasthan, Jaipur, Rajasthan, India, for providing over all support and the necessary laboratory facilities to fulfill the present research work. Financial support of this work has been provided by the CSIR-UGC, New Delhi, NTA Ref. No.: 201610163511.

| ®úÇí

öÖı¼—‰óıøı ł—–ŁŒø— G ß— œ Œû—ßı ¬ł— ı œ ı ł°¹óÖ°öłÖö°ß— ó ª¹‰óÖª—
œ —ŁßŒæı‰öœ –¹ łóı ûø¹°ı Ø—

NISHA YADAV[1],BHUPENDRA PAL[2] | MEENAKSHI[1]

[1]Ddo‘qsl dmsneBgdl hnsqx,Umhudqrhsx neR‘i‘nsg‘m,I‘hotq,R‘i‘nsg‘m,2/2//3,Imch‘ | [2]Gnudqml dms Pnkssdbgmhb Bnkkdfd,K‘q‘tkh,R‘i‘nsg‘m,222231,Imch‘

œ ½ëÁÐ®| ŮÝ -ÇþÅ|ŠÃÇð|íÁ| õÐýÐÁµ (œ ¹B),úðÅµ½óÇðÐÃ õÐýÐÁµ½,ñÇÁçúÇ ÐíÇÕ|Ç Á½ ®Á½Ñ½ŮÞ½Ç ÇíõÎ |ú| ëõ½›Ðú|ÁÅþ| ý½µÐ| ¼Ã ®ÕÇéý½ÃÇéÙé, ÐÁ|ÑÁÇéÇµ|Åþ½ | ý½ÃÐ ñÇuðÇ-Ú″Ð ÐÁÐõé| Ð. œ Ð›Ùµ|ý , ñð|ýÐÁ½ ÇúÇé õÐýÐÁµ½ Ù ëõ½›Ðú|Á½õÅuúÙ ÇÅµ½Ð Çëõ½Á|ÑÐÁ½, ñðúÐÁÅuúÐÁÇ ®ÕÇé ÁÐ½íÐþú½µÁÐ ÇuñÇðÁÇÅµ| Á½ úÃ½ëÙ | ý½ÃÐ ñÇÑÐµÁÐ ÑúðÅuÇ»Ð Á½ ñÇú|-ÚÐÁ|ý µÐýñÐõ½µÙõ½ý½.ö ÇúÇý õ½íÙ Ð |Åñ|µ|ú½Á Ùµ|õ½ˇõ½®Ã|Ñ|µ|Š þÇÃ|Ñ|Á½Å|Ã|þ½ëÐÃ½ G (/·2/ý½Å.% SG)Á½ÅúÇŮuú½íÇÕ| ŮÁ|Š þÇýñÇ®|µ½œ ¹B·SG .—Á½Ã|®|õ½Á½ÅÙÈ |®|Ñþ½ | ýÐŠ½Á|Ñþ½ ÅúÇŮuú½ Çú|Š þÇýñÇ®|µ½, Ùþ, ÙÑÙÙ»| úðÐýÐ úÐ®|ú½″½, ÇuñÇðÁÇÅµ Á½ úÃ½ëÙ | ÑúðÅuÇ»Ù Á½ñð|µ|Å½þ.– ÇðÐí µÇé½,ÅñðÇúÐíÐÁÐ ÅÙ | FTIR,XRD,SEM-EDX | TGA ½Á½Ã|®Ð þ½þÇ Õ| ÅÐ |Åñ|µ½ÃÐ þð|Åµ½ÃÁÐ È½®Ð þÇýñÇ®|µ½ | ÅuðÙþuÙðÁÐ þ½õ½þuÐð|Åµ|þÐ.SG íÐÃÙÐ þ½Ç úÐ®|úÁÇ ÅðÐíÅuúÇ, ñÇúÐ»½ú½Ù» | Ñúðuµ|ÇÙ | |®íõî , |úÇÅµ þÇýñÇ®|µ½.¹úÇ |Åuð½î |-ú½″Ð ñÇþ½®ÙÐ ñÇuÐÁõ|¼Ã þÇýñÇ®|µ½œ ¹B·SG þ½Ç ÇÕÐ»½ú½Ù»Ðé Çíõî |úÇé ëõ½›Ðú|ÁÅþÇé ý½µÐð|¼Ã½.°Ð®ÙÃµ½µ| ñÇþ½®ÙÙí½íÇí½ú½″Ð5% SG ®Á½Ñ½ÁÇ ñÇÕÇ,Ú½ú½ÅúÇŮuú½MOB.

(–ð|ý,ÐÁÇ17.íÐõÐý Õð½2/25,ðÐú|í|ð½ÁÇ19.¼ÁÙ½ð½,ñð|Šú½»ÐÁÇ21.½ñð|Ã½2/26)

REFERENCES

1. A. Bentur, *J. Mater. Civ. Eng.* **14** (2002) 2 (https://doi.org/10.1061/(ASCE)0899--1561(2002)14:1(2))
2. S. T. Sorel, *Comptes Rendus hebdomadaires des Séances de l'Académie des Sciences, Paris, France* **65** (1867) 102 (https://gallica.bnf.fr/ark:/12148/bpt6k3022r/f104.item)
3. S. A. Walling, J. S. Provis, *Chem. Rev.* **116** (2016) 4170 (https://doi.org/10.1021/acs.chemrev.5b00463)

4. D. Meng, C. Unluer, E. H. Yang, S. Qian, *Cem. Concr. Compos.* **138** (2023) 104983 (https://doi.org/10.1016/j.cemconcomp.2023.104983)
5. W. Shen, L. Cao, Q. Li, Z. Wen, J. Wang, Y. Liu, R. Dong, Y. Tan, R. Chen, *J. Clean. Prod.* **131** (2016) 20 (https://doi.org/10.1016/j.jclepro.2016.05.082)
6. L.Wang, L. Chen, D.C.W. Tsang, in *Sustainable Remediation of Contaminated Soil and Groundwater*, D. Hou, Ed., Butterworth-Heinemann, Oxford, 2020, pp. 93–118 (https://doi.org/10.1016/B978-0-12-817982-6.00005-7)
7. M. Costato, *Nuovo Cimento, D* **17** (1995) 545 (https://doi.org/10.1007/BF02451742)
8. A. Maier, D. L. Manea, *Materials* **15** (2008) 1772 (https://doi.org/10.3390/ma15051772)
9. Q. Huang, W. Zheng, J. Dong, J. Wen, C. Chang, X. Xiao, *J. Build. Eng.* **57** (2022) 104923 (https://doi.org/10.1016/j.jobe.2022.104923)
10. R. N. Yadav, P. Gupta, *Adv. Cem. Res.* **26** (2014) 319. (http://dx.doi.org/10.1680/adcr.13.00036)
11. Meenakshi, *Asian J. Chem.* **35** (2023) 869 (https://doi.org/10.14233/ajchem.2023.26992)
12. N. Zhang, H. Yu, H. Ma, H. Ma, M. Ba, *Composites, B* **247** (2022) 110328 (https://doi.org/10.1016/j.compositesb.2022.110328)
13. Y. Guan, Z. Hu, Z. Zhang, J. Chang, W. Bi, C. R. Cheeseman, T. Zhang, *Cem. Concr. Res.* **143** (2021) 106387 (https://doi.org/10.1016/j.cemconres.2021.106387)
14. R. A. S. Alatawi, N. H. Elsayed, W. S. Mohamed, *J. Mater. Res. Technol.* **8** (2019) 244 (https://doi.org/10.1016/j.jmrt.2018.01.010)
15. C. Guo, N. Chen, R. Wang, *J. Build. Eng.* **98** (2024) 111070 (https://doi.org/10.1016/j.jobe.2024.111070)
16. C. Li, N. Zhou, P. Guo, M. Li, F. Wang, J.Li, Y. Han, Z. Wu, W. Lu, *Adv. Compos. Hybrid Mater.* **8** (2025) 43 (https://doi.org/10.1007/s42114-024-01129-5)
17. Y. Li, Z. Li, H. Pei, H. Yu, *Constr. Build. Mater.* **102** (2016) 233 (https://doi.org/10.1016/j.conbuildmat.2015.10.186)
18. B. Şimşek, *Constr. Build. Mater.* **320** (2022) 126250 (https://doi.org/10.1016/j.conbuildmat.2021.126250)
19. Y. Yin, J. Huang, T. Wang, R. Yang, H. Hu, M. Manuka, F. Zhou, J. Min, H. Wan, D. Yuan, B. Ma, *Constr. Build. Mater.* **405** (2023) 133347 (https://doi.org/10.1016/j.conbuildmat.2023.133347)
20. Z. Qin, J. Wu, Z. Hei, L. Wang, D. Lei, K. Liu, Y. Li, *Materials* **17** (2024) 2053 (https://doi.org/10.3390/ma17092053)
21. L. Wang, Z. Qin, J. Wu, G. Sheng, H. Wang, K. Liu, X. Dong, F. Wang, J. Jiang, *Buildings* **14** (2024) 41 (https://doi.org/10.3390/buildings14010041)
22. M. Harun, U. Ali, M. Aziz, M. A. Mohamed, H. R. Khalid, S. Ahmad, A. Hanif, *Res. Eng.* **27** (2025) 105915 (https://doi.org/10.1016/j.rineng.2025.105915)
23. F. Ahmed, S. Rawat, Y. Zhang, *Appl. Sci.* **14** (2024) 3074 (https://doi.org/10.3390/app14073074)
24. H. M. Hamada, A. Al-Attar, M. K. Askar, S. Beddu, A. Majdi, *Int. J. Concr. Struct. Mater.* **19** (2025) 76 (https://doi.org/10.1186/s40069-025-00808-x)
25. H. Zhang, A. Luo, L. Sun, *Sci. Rep.* **14** (2024) 11656 (https://doi.org/10.1038/s41598-024-62602-1)
26. W. Chen, C. Wu, F. Chen, S. Zheng, in *Proceedings of the 2017 6th International Conference on Energy and Environmental Protection*, 2017, pp. 1251–1254 (https://doi.org/10.2991/iceep-17.2017.219)
27. Y. Guo, Y. X. Zhang, K. Soe, R. Wuhrer, W. D. Hutchison, H. Timmers, *J. Cleaner Prod.* **313** (2021) 127682 (https://doi.org/10.1016/j.jclepro.2021.127682)

28. A. Pivák, M. Pavlíková, M. Záleská, M. Lojka, O. Jankovský, Z. Pavlík, *Materials* **13** (2020) 2537 (https://doi.org/10.3390/ma13112537)
29. M. S. Elfeky, A. Mohsen, A. Maher, M. Kohail, *Const. Build. Mat.* **342** (2022) 127976 (https://doi.org/10.1016/j.conbuildmat.2022.127976)
30. Q. Huang, W. Zheng, X. Xiao, J. Dong, J. Wen, C. Chang, *Ceramics Int.* **47** (2021) 34341 (https://doi.org/10.1016/j.ceramint.2021.08.347)
31. IS 11803 – 1986: *Magnesium oxide for explosive ammunition protective compositions and pyrotechnic industry*, 1986
32. IS 254 – 1973: *Specification for magnesium chloride*, 1973
33. IS 10132 - 1982: *Method of test for materials for use in the preparation of magnesium oxychloride flooring compositions*, 1982
34. R. E. Dinnebier, I. Halasz, D. Freyer, J. C. Hanson, *Z. Anorg. Allg. Chem.* **637** (2011) 1458 (https://doi.org/10.1002/zaac.201100139)
35. T. Zhang, Q. Guo, X. Chen, C. Cheeseman, H. Wang, J. Chang, *Cement Conc. Compos.* **157** (2025) 105941 (https://doi.org/10.1016/j.cemconcomp.2025.105941)
36. E. A. Paukshtis, M. A. Yaranova, I. S. Batueva, B. S. Bal'zhinimaev, *Micropor. Mesopor. Mat.* **288** (2019) 109582 (https://doi.org/10.1016/j.micromeso.2019.109582)
37. Y. Hao, Y. Li, *Constr. Build. Mater.* **282** (2021) 122708 (https://doi.org/10.1016/j.conbuildmat.2021.122708).

Journal of the Serbian Chemical Society
JSCS-info@shd.org.rs • www.shd.org.rs/JSCS
J. Serb. Chem. Soc. 91 (0) S1–S3 (2026) *Supplementary material*

SUPPLEMENTARY MATERIAL TO

Impact of silica gel G on mechanical and microstructural properties of magnesium oxychloride

NISHA YADAV[1], BHUPENDRA PAL[2] and MEENAKSHI[1]*

[1]*Department of Chemistry, University of Rajasthan, Jaipur, Rajasthan,302004, India and* [2]*Government Polytechnic College, Karauli, Rajasthan, 322241, India*

J. Serb. Chem. Soc. 91 (0) (2026) 000–000

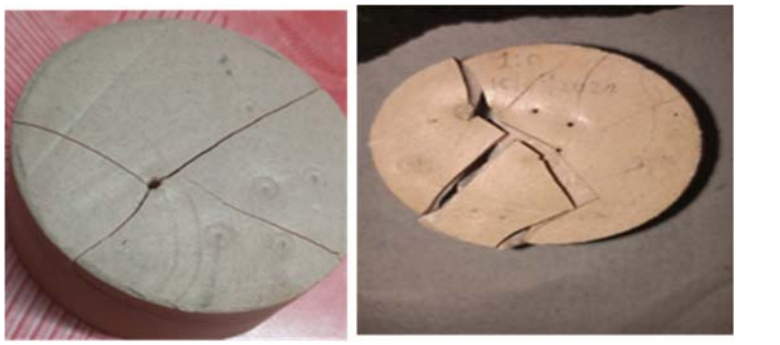

(a)

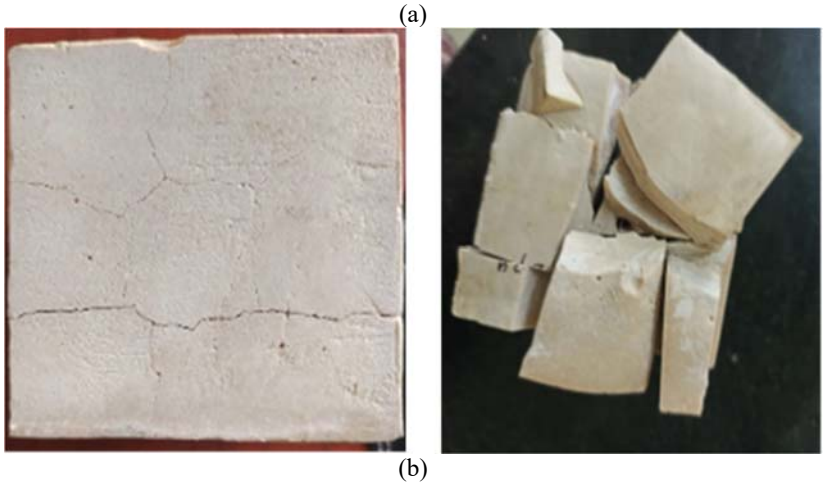

(b)

Fig. S-1. Cracking in setting time blocks (a), and in compressive strength blocks (b).

* Corresponding author. E-mail: meenakshialwaraj@gmail.com

Fig. S-2. Compressive and setting time blocks without cracking.

Fig. S-3. Compressive strength testing of MOC block by UTM machine.

528 Table S-I: Compressive strength sample preparation.

Sample no.	Silica Gel G (SG)		MgO (g)	Dolomite (g)	Gauging solution (mL)
	(%)	(g)			
M0	0%	0	540	0	209.3
M1	0%	0	270	270	169.5
SG1	5%	13.50	270	270	207.50
SG2	10%	27.00	270	270	220.00
SG3	15%	40.50	270	270	239.90
SG4	20%	54.00	270	270	248.10

529

530 Table S-II: Setting time sample preparation.

Sample no.	Silica Gel G (SG)		MgO (g)	Dolomite (g)	Gauging solution (mL)
	(%)	(g)			
M0	0%	0	200	0	78.9
M1	0%	0	100	100	72.2
SG1	5%	5.00	100	100	76.00
SG2	10%	10.00	100	100	79.60
SG3	15%	15.00	100	100	84.20
SG4	20%	20.00	100	100	100.60

531 Table S-III: Water resistance of M0, M1, and different types of MOC-SG samples.

Composition	Different types of MOC blocks immersed in boiling water for					
	0-5 hours	5-10 hours	10-15 hours	15-20 hours	20-25 hours	25-30 hours
M0	During curing M0 was cracked					
M1	N	N	N	N	N	N
SG -1	N	N	N	N	N	N
SG- 2	N	N	N	N	N	N
SG- 3	N	N	N	N	N	N
SG- 4	N	N	N	N	N	N

532 N = Not affected